Selenium−Tellurium Sequences in Binary Glasses as Depicted by ^{77}Se and ^{125}Te NMR

Bruno Bureau,* Catherine Boussard-Plédel, Marie LeFloch, Johann Troles, Frédéric Smektala, and Jacques Lucas

Laboratoire des Verres et Céramiques, UMR-CNRS 6512, université de Rennes 1, campus de Beaulieu, 35042 Rennes Cedex, France

Received: December 9, 2004; In Final Form: February 8, 2005

Some resolved solid state ^{77}Se NMR spectra are presented in the Te_xSe_{1-x} vitreous system at ambient temperature. They exhibit three different kinds of Se lines assigned to the following **Se** atom neighborhoods: Se-**Se**-Se, Se-**Se**-Te, and Te-**Se**-Te. Different models were considered to describe the way the Se and Te atoms are linked into the chains: clustering process, homogeneous distribution, random distribution. Finally, thanks to the measurements of the relative intensities of the lines, it appears that Se and Te atoms are mainly randomly distributed with a small preference for heteropolar bonds. The ^{125}Te spectra are also shown but their resolution is too weak to be informative concerning the vitreous network.

1. Introduction

Compared to oxide-based glasses, vitreous materials involving chalcogens form an original family of glasses which have received attention, mainly because of their transmission in the mid infrared. These low phonon materials have to be considered as heavy anion glasses since sulfur (S), selenium (Se), and also tellurium (Te) are the main constituents of their compositions. This situation leads to fundamental vibrational modes shifted far in the IR, rending these glasses interesting for the fabrication of thermal imaging systems.[1] Some selected compositions of these low phonon glasses are very resistant to devitrification and can be drawn into optical fibers which offer an exceptional spectral window.[2−5] It must be noticed that these chalcogenide glasses contain large polarizable atoms associated with external lone pair electrons and are prone to exceptional nonlinear optical properties when irradiated by an electromagnetic field. Then, they are also serious candidates for fast switching and signal regeneration devices for telecommunications.[6−8]

A good knowledge of the glass structure is essential to understand some mechanical, optical, and chemical properties of such materials, and the difficulties associated with the disordered nature of the glassy state are a real challenge. To achieve this goal, it appears essential to understand the behavior of the Se and Te atoms into the binary Te_xSe_{1-x} vitreous system. Recently, similar works have been carried out for the As_xSe_{1-x} and Ge_xSe_{1-x} glasses.[9−12] These studies related to binary systems have to be considered also as a first step toward a better understanding of more complicated glassy network such as TeAsSe and GeAsSe systems, for example. In the Te_xSe_{1-x} glasses, Te and Se atoms are both 2-fold coordinated, and then the network is assumed to be built of chains. Thus, ^{77}Se together with ^{125}Te NMR experiments are potentially very informative to model this vitreous structural network. As far as Se-containing glasses are concerned, ^{77}Se NMR spectroscopy appears to be a powerful method to obtain indications on the local Se environment, which contributes to reinforce the construction of structural models.[9−14] Nevertheless, the ^{77}Se natural abundance (7.58%), its low relative sensitivity (6.93×10^{-3}), together with its long longitudinal relaxation time make these NMR experiments time-consuming and rend this nucleus very rarely studied in solid-state inorganic materials.[9−14]

The isotropic component of the ^{77}Se chemical shift interaction tensor δ_{iso} is very sensitive to the neighborhood of the Se atoms, and values lying from −900 ppm to +2430 ppm can be measured.[14] It will be shown that these experiments allow us to find evidence for three Se environments which are well characterized and quantified, leading to a precise description of the glassy network. These results are coupled with ^{125}Te NMR experiments, which are unfortunately not very informative. Nevertheless, such ^{125}Te acquisition in solid-state inorganic materials remains quite rare,[15−20] and the recorded spectra will also be shown in the Te_xSe_{1-x} glasses and in the crystalline phase of pure Te (c-Te).

2. Experimental Section

2.1. Materials. The glasses are prepared from ultrapure elements with 99.999% elemental purity. Selenium is purified of remaining oxygen by distillation under vacuum at 250 °C and tellurium by surface cleaning treatment. The required amounts of Se and Te are heated at 600 °C for 12 h in an evacuated silica ampule, then placed in a rocking furnace for homogenization. The ampules are then quenched in air and annealed near glass transition temperatures (T_g) to reduce the mechanical stresses occur by the fast cooling. Note that the synthesis was performed using an ampule with lower diameter than usual (about 5 mm) to ensure a homogeneous vitrification of the mixture due to faster heat transfer during quenching. The glassy nature was confirmed by X-ray diffraction and differential scanning calorimetry (DSC). The values of T_g are 45 °C (pure g-Se), 55 °C ($SeTe_9$), 66 °C ($SeTe_4$), 67 °C ($SeTe_3$), 69 °C ($TeSe_2$), and 72 °C (TeSe). Beyond this stoichiometry, it has not been possible to fabricate vitreous samples in the given quenching conditions.

2.2. NMR Measurements. The ^{77}Se and ^{125}Te ($I = 1/2$) NMR spectra were recorded at room temperature on an ASX 300 Bruker spectrometer operating respectively at 57.3 and 94.8 MHz with a 4 mm MAS probe spinning at 15 kHz. The spectra

* Corresponding author. E-mail: bruno.bureau@univ-rennes1.fr, tel: 33 (0)2 23 23 65 73, fax: 33 (0)2 23 23 56 11.

10.1021/jp044398n CCC: $30.25
Published on Web 03/11/2005

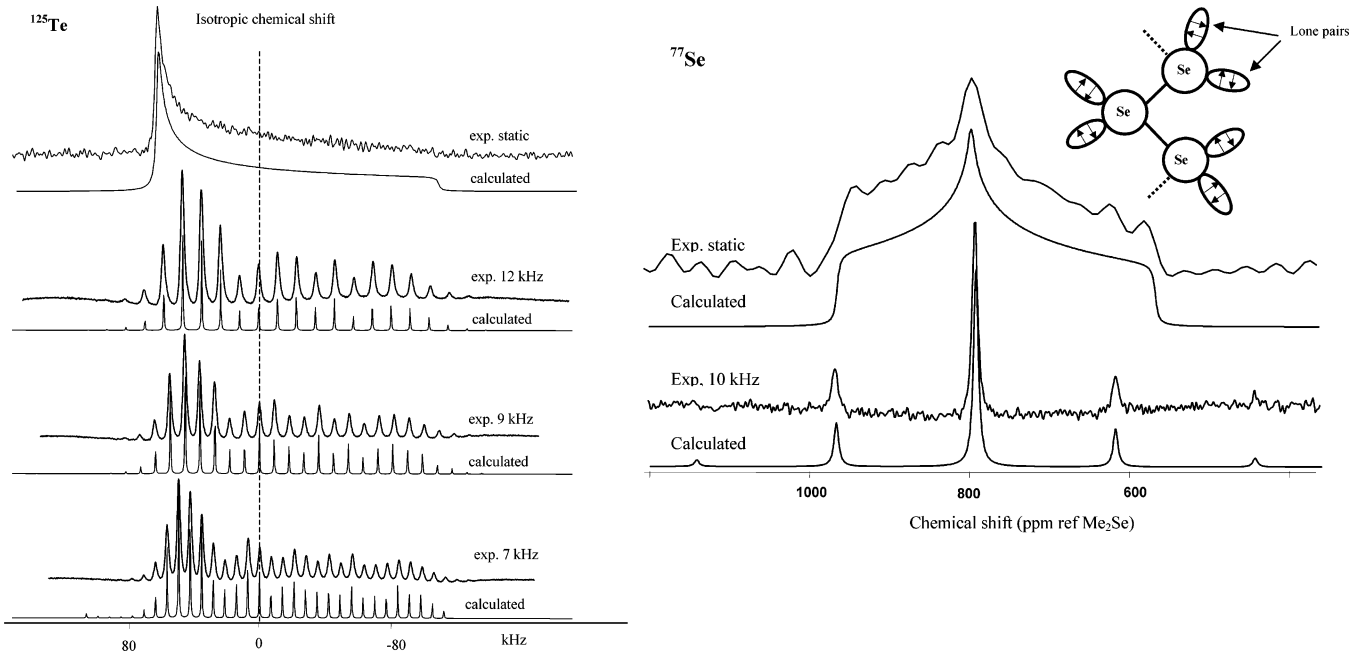

Figure 1. (a) ^{125}Te MAS and static NMR spectra in the crystalline phase of pure Te exhibiting a perfect axial symmetry. (b) ^{77}Se MAS and static NMR spectra in the crystalline phase of pure Se.

were recorded with the maximum spinning speed reachable (15 kHz) to reduce the dipolar interaction that is expected to be weak in view of the low abundances and sensitivities of both nuclei (respectively 7.58%, 5.25×10^{-4} for ^{77}Se and 7%, 2.2×10^{-3} for ^{125}Te). So, the remaining broadness of the lines is due to the isotropic chemical shift distributions characteristic of the vitreous states. Moreover, due to this strong residual broadness of the lines (about 80 kHz for both nucleus), a Hahn spin−echo sequence was implemented to refocus the whole magnetization and to avoid any distortion of the baseline. The Fourier transformation was done from the whole echos (so-called full-shifted echos) in order to increase the signal-to-noise ratio and overall to directly obtain some absorption mode line shapes.[21,22] The processing and acquisition parameters were: 3.5 μs $\pi/2$ pulse duration (7 μs for the π pulse), 30 s recycle time, spectral width 1 MHz, time domain 1 K. To ensure that MAS together with spin−echo acquisition do not cause any distortion of the line shapes, we have to choose a time delay between the pulses equal to $1/\nu_R$ where ν_R is the spinning speed. So the 15 kHz MAS spectra were recorded with a delay of 67 μs. Owing to the weak sensibility of both nuclei, about 10 000 scans were necessary to obtain a sufficient signal-to-noise ratio. The external reference used for the selenium chemical shifts is Me_2Se in $CDCl_3$.[14] For the tellurium, the crystalline phase of pure Te was positioned at 0 ppm (292 ppm from aqueous $Te(OH)_6$[15]). The simulations of the experimental spectra were performed using the Dm2000nt version of the Winfit software.[23]

3. Results

The first experiments were carried out on the crystalline phases of pure selenium and tellurium, c-Se and c-Te. For both crystals, the crystalline hexagonal lattice is made of spiral chains of atoms, each of them being 2-fold coordinated, with two lone pair electrons remaining unbounded.[24] Each MAS spectrum exhibits a unique line in agreement with the structural data. The static spectra exhibit a broadened shape due to the chemical shift anisotropy. The experimental MAS and static spectra are plotted in Figure 1 together with the reconstructed spectra. A chemical shift anisotropy line shape model provides spectra that fit simultaneously well the experimental ones using the same set of parameters for static and MAS acquisitions (Table 1). Note that the measured asymmetry parameters are very different for Te and Se, although they belong to the same structural model. Indeed, the geometry of the electronic cloud around Te and Se atoms is also very different since tellurium conducts electricity due to its low band gap ($\Delta = 0.32$ eV), whereas selenium is an electrical insulating material possessing a large electronic gap ($\Delta = 0.32$ eV).[25] Then for c-Te, a fraction of the lone pair electrons are delocalized along the σ bonded chains, and the axial symmetry observed, in agreement with ref 15, is attributed to this axial electronic motions. Note that the anisotropy measured is much smaller than that obtained in ref 15 (−1100 ppm instead of −1800 ppm). On the other hand, the lone pair electrons of Se atoms in c-Se provide a complex local symmetry justifying the higher η value measured in this crystal. Finally, the quality of the fits together with the full agreement between the parameters used for both reconstructions, static and MAS, confirms our ability to record reliable ^{77}Se and ^{125}Te spectra in inorganic solid-state materials.

TABLE 1: Parameters Used for the Reconstruction of the Se and Te Crystalline Phases: $\delta_{iso} = 1/3(\delta_{xx} + \delta_{yy} + \delta_{zz})$, $\delta_{aniso} = \delta_{zz} - \delta_{iso}$, and $\eta = (\delta_{yy} - \delta_{xx})/\delta_{aniso}$

name	c-Se	c-Te
isotropic chemical shifts δ_{iso} (± 5 ppm)	800	0
anisotropy δ_{aniso} (± 10 ppm)	−250	−1160
asymmetric parameter η	0.8	0

The ^{77}Se 15 kHz MAS NMR spectra for the six vitreous materials are compared in Figure 2. Despite the weak signal-to-noise ratio, three types of line positions are clearly visible at about 880 ppm (labeled a), 710 ppm (labeled b), and 510 ppm (labeled c) for the chemical shift values. The a line is assigned to selenium bonded to two other selenium, noted Se-**Se**-Se, as in the crystalline and vitreous phases of pure Se. Then, as observed for previous glassy systems,[9−11] the b and c lines are respectively assigned to Se-**Se**-Te and Te-**Se**-Te.

Then the spectra were reconstructed using the Winfit Bruker software[23] thanks to Gaussian contributions for each line as shown in Figure 3 for $TeSe_4$. The parameters of the reconstruc-

TABLE 2: Parameters Used for the Glass Sepctrum Reconstructions[a]

name	Se			$TeSe_9$			$TeSe_4$			$TeSe_3$			$TeSe_2$			TeSe		
x values (Te_xSe_{1-x})	0			0.1			0.2			0.25			0.33			0.5		
compositions	100% Se			90% Se			80% Se			75% Se			66% Se			50% Se		
	0% Te			10% Te			20% Te			25% Te			33% Te			50% Te		
lines	a	b	c	a	b	c	a	b	c	a	b	c	a	b	c	a	b	c
chemical shifts (±10 ppm)	65	-	-	80	700	-	880	700	510	880	700	500	860	690	500	900	710	510
relative intensities (±5%)	100	0	0	75	25	0	55	40	5	45	50	5	30	55	15	15	45	40

[a]Three type of lines, noted a, b and c, are evidenced and attributed as explained in the text.

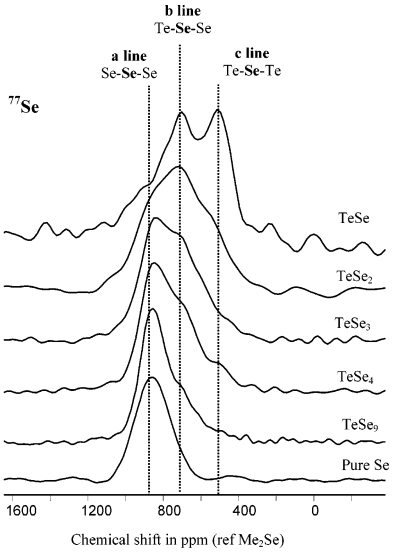

Figure 2. ^{77}Se NMR MAS (15 kHz) spectra of Te_xSe_{1-x} glasses exhibiting three types of line labeled *a*, *b*, and *c*, respectively, assigned to Se-**Se**-Se, Se-**Se**-Te, and Te-**Se**-Te.

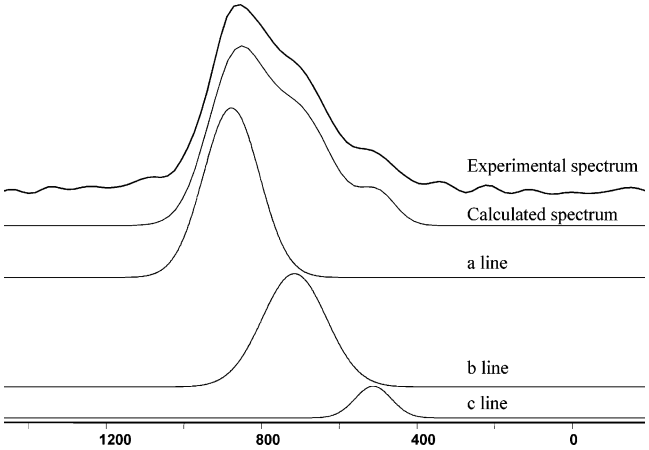

Figure 3. Reconstruction of the ^{77}Se MAS (15 kHz) spectrum of $TeSe_4$ glass with three Gaussian contributions. The integrated intensities of the three lines give the proportion of the Se-**Se**-Se, Se-**Se**-Te, and Te-**Se**-Te in the glass.

tion are given in Table 2. The three contributions remain at the same chemical shift values for all glasses, confirming the presence of three types of Se neighborhoods. It appears that the changes in relative intensities are in agreement with the above assignments: the higher Te content in the glass composition produces a higher intensity of the b and c line and a lower intensity of the a line (see Table 2).

Concerning the ^{125}Te, the spectra recorded in the glasses are too unresolved to be informative (Figure 4). Moreover, given the large chemical shift anisotropy, the glass spectra undergo overlapping of the spinning sidebands. The barycenters of these broad lines are shifted toward 0 ppm (position of c-Te) for the richer in tellurium glass compositions.

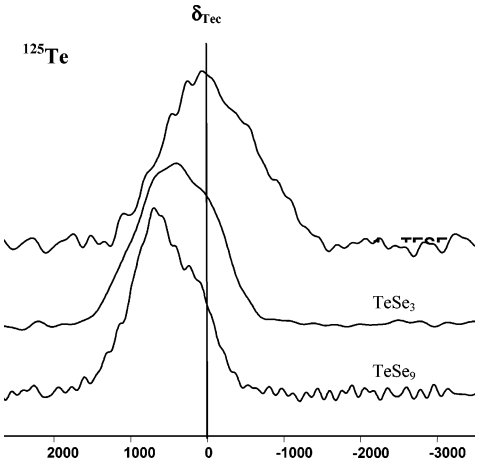

Figure 4. ^{125}Te NMR MAS (15 kHz) spectra of Te_xSe_{1-x} glasses. The unresolved broad line shifts toward δ_{Tec} for the richer composition in Te.

4. Discussion

In view of the lack of information provided by ^{125}Te spectra, the discussion is based on the ^{77}Se results. In view of the previous similar works on Ge_xSe_{1-x} and As_xSe_{1-x} vitreous systems, two structural models have to be considered for the Se-enriched compositions.[9,10]

The first model reckoned the existence of clusters constituted of $GeSe_4$ tetrahedra gathered and shared by bridging Se, releasing the surplus Se to form chains or rings.[9] For Te_xSe_{1-x} glasses, the equivalent model would lead to pieces of −Te−Se−Te−Se− chains on one hand (Te atoms being 2-fold coordinated) coexisting with Se−Se−Se chains on the other hand, and the glass formula could be rewritten as $TeSe_{1-x/x} = TeSeSe_{1-2x/x}$. Then we would obtain $100 \cdot x/(1-x)$ of Te-**Se**-Te, $100 \cdot (1-2x)/(1-x)$ of Se-**Se**-Se, and no Se-**Se**-Te. This network description is clearly unsuitable since the NMR spectra exhibit three lines with integrated intensities very far from the above percentages. Another way to view the clustering process would be to consider a total phase separation between Te atoms and Se atoms, providing 100% of Se-**Se**-Se, regardless of the x values. Once again, this network description is in total disagreement with the experimental data.

The second model, known as the "chains crossing model", was well adapted to give account of the As_xSe_{1-x} vitreous network.[10] It consists of considering that the As atoms are homogeneously distributed throughout the network. In the present case, it would give rise to Te atoms connected to each other by pieces of Se chains having the same length. The number of Se between two Te depends on the initial compositions: the richer the composition in Se, the longer are the chains. For example, $TeSe_2$ is built up with −Te−Se−Se−Te− patterns, $TeSe_3$ with −Te−Se−Se−Se−Te−, etc. Note that this model is in favor of the largest average distances between Te atoms and privilege thus exclusively heteropolar bonds. From pure Se to $TeSe_2$ ($x = 0$ to $x = 0.33$) the glass formula can be

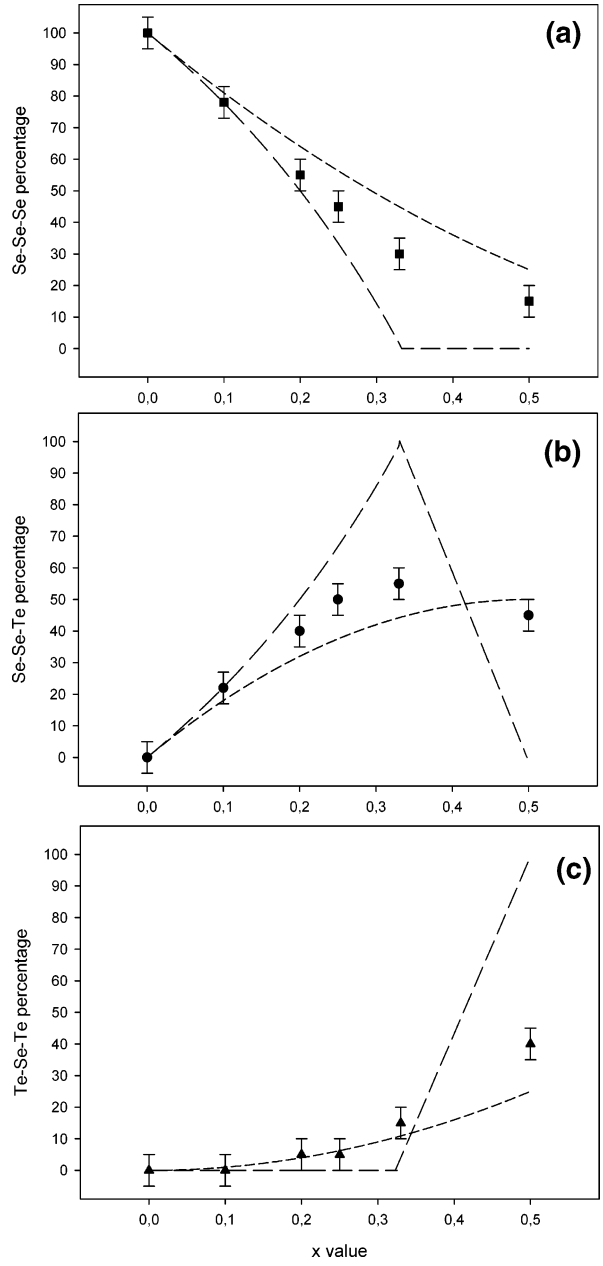

Figure 5. Comparison between the *a*, *b*, and *c* line-normalized intensities (respectively Figure 5a, 5b, and 5c) and the expected Se-**Se**-Se, Te-**Se**-Se, and Te-**Se**-Te ratios with the "chain-crossing model" (long dashed lines) and a random distribution (short dashed lines). The experimental data have intermediate positions between the both models.

rewritten as $Te_xSe_{1-x} = TeSe_2Se_{1-3x/x}$, and only two types of Se atoms are expected: $200x/(1-x)$ of Te-**Se**-Se and $100(1-3x)/(1-x)$ of Se-**Se**-Se. Then, from $TeSe_2$ to TeSe, Se-**Se**-Se should vanish and the rate of Te−Se−Te increases linearly to the detriment of the Te-**Se**-Se rate. Figure 5 shows a large discrepancy between experiments and these calculated intensities, disqualifying consequently the "chains crossing model".

A third scenario consists of a random distribution of Te and Se atoms into the chains. This kind of behavior has already been considered in high-temperature liquid phases of As_xSe_{1-x} glasses.[12] In our case the calculations are easy since Te and Se are both 2-fold coordinated. Then, for Te_xSe_{1-x} the probabilities to have Te-**Se**-Te, Se-**Se**-Te, and Se-**Se**-Se are, respectively, $100x^2$, $200x\cdot(1-x)$, and $100(1-x)^2$. Figure 5 shows that the agreement is better than with the previous model but still far from being perfect. Indeed, the experimental data have intermediate positions between both previous models.

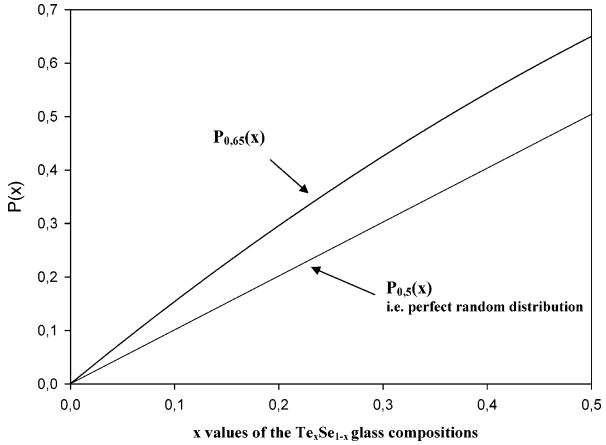

Figure 6. Plot of the $P_k(x)$ polynomial expression $P_k(x) = x[(0.5-k)/0.25x + (k-0.25/0.25]$ for $k = 0.5$ and 0.65. This polynomial expresses the probabilities to have a Te atom connected to a Se atom. $P_{0.5}(x) = x$ is a straight line meaning that the probability is directly equal to the Te rate in the composition as expected with a perfect random distribution of the both types of atom. $P_{0.65}(x)$ is a second degree polynomial that enables to privilege the heteropolar Se−Te bonds compared to a pure random distribution.

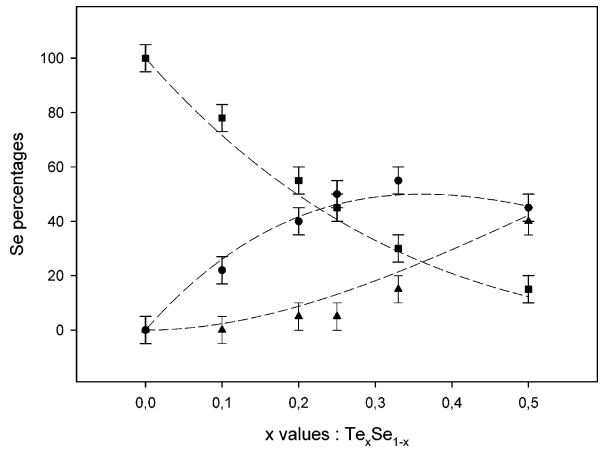

Figure 7. Comparison between the *a*, *b*, and *c* line-normalized intensities (respectively, square, circle, and triangle) and the calculated Se-**Se**-Se, Te-**Se**-Se, and Te-**Se**-Te percentages calculated using $P_{0.65}(x)$: $100P_{0.65}^2(x)$ for the Te-**Se**-Te line intensity, $200P_{0.65}(x)(1-P_{0.65}(x))$ for Se-**Se**-Te, and $100(1-P_{0.65}(x))^2$ for Se-**Se**-Se.

So it appears that a compromise has to be found between an ideal dilution and a random distribution of Te and Se atoms. For this, instead of considering that the probability to meet Te connected to Se is simply given by $P(x) = x$, as in the above random distribution, we have improved the model by considering this probability equal to a second degree polynomial $P_k(x)$. Here, k is a parameter defined as $P_k(0.5) = k$ that has to be fit with the experimental data. Knowing that $P(0) = 0$ and $P(1) = 1$, we thus obtain $P_k(x) = x[(0.5-k)/0.25x + (k-0.25)/0.25]$. This polynomial is the simplest mathematical law to express a probability in agreement with the above schedule of conditions. The k value express the probability to have Te connected to Se in an equimolar mixture ($x = 0.5$). Consequently for $k > 0.5$, heteropolar bonds (Te−Se) are privileged, and for $k < 0.5$, homopolar bonds (Se−Se) are privileged. For $k = 0.5$, the previous perfect random distribution is retrieved: $P_{0.5}(x) = x$. In Figure 6, $P_k(x)$ is plotted for $k = 0.5$ and $k = 0.65$. Indeed, as shown in Figure 7, the best fit between experiments and calculation is obtained for $k = 0.65$. The rates of Se for each

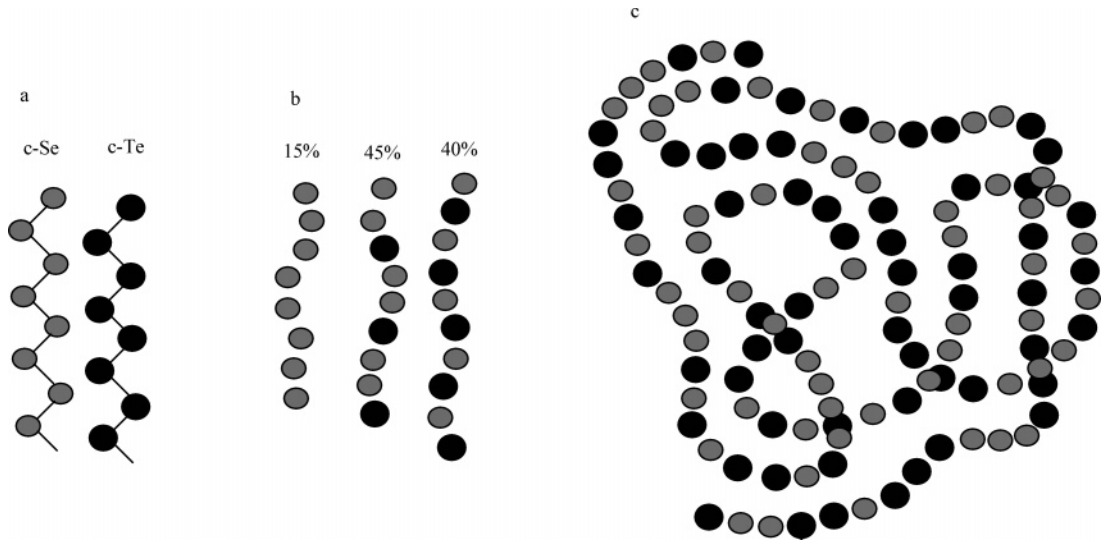

Figure 8. Reconstruction of the TeSe vitreous network. From the same amount of c-Te and c-Se (Figure 8a) in the glass composition, the NMR data foresee the presence of the sequences depicted Figure 8b. Figure 8c is then an example of linking of pieces of the previous sequences that give rise to numerous unavoidable Te−Te bonds. For the richer compositions in Te, the Te−Te fragments are assumed to be rather out of the chains and spread in the glassy matrix.

type are given by $100P_{0.65}^2(x)$ for Te-**Se**-Te, $200P_{0.65}(x)\cdot(1 - P_{0.65}(x))$ for Se-**Se**-Te, and $100(1 - P_{0.65}(x))^2$ for Se-**Se**-Se. The good agreement observed in Figure 7 means that for a mixture containing the same amount of Se and Te atoms ($x = 0.5$), the probability to have Te around Se is 65% and only 35% for Se. Finally, the Te and Se linking is mainly governed by a random process where the heteropolar bonds have nevertheless to be privileged.

This conclusion implies that direct Te−Te bonds have to be assumed, especially for the richer composition in tellurium. Unfortunately, the weak resolution of the ^{125}Te spectra do not permit to directly quantify the amount of such bonds. Nevertheless, from the ^{77}Se results it is possible to evaluate the rate of Te atoms that are connected to other Te atoms. For example, the TeSe glass spectrum reconstruction led to 15% for Se-**Se**-Se, 45% for Se-**Se**-Te, and 40% for Te-**Se**-Te (Table 2). Moreover, each Se-**Se**-Se does not see any Te in infinite ...Se−Se−Se−Se... strings, 45% of Se-**Se**-Te provide 45/2% of Te in ...Te−Se−Se−Te−Se−Se−Te... strings, and 40% of Te-**Se**-Te give 40% of Te in ...Te−Se−Te−Se... sequences. So, the glass formula as obtained from the NMR measurements is $Te_{0,625}Se$ instead of TeSe, meaning that about 37.5% of the Te atoms introduced in the initial glass composition are not only connected to Se atoms but are also linked to at least one Te. This rate falls to 15% for $TeSe_2$ (using the same reasoning), 10% for $TeSe_3$, and becomes null for $TeSe_4$. These calculations are coherent with Figure 4 where it is shown that the ^{125}Te broad line is shifted toward the chemical shift of the c-Te phase when the Te rate increases in the initial composition. As an example, a TeSe glass network model is proposed in Figure 8 using the above discussion results. As depicted by the selenium−tellurium sequence, a large amount of Te−Te bonds have to be introduced in order to respect the NMR data.

The differences between the electronic and bonding behaviors of both crystals, c-Se and c-Te, have been clearly pointed out by their respective NMR spectra presented in Figure 1 (see discussion in section 3 and in ref 25). Consequently, from our point of view, the introduction of ...Te−Te... fragments inside the chains of the glass network seems inconsistent with the strong bonding existing in the c-Te, which is attributed to the addition of σ bonds plus delocalized metallic π bonding. Clearly, the Te chains have a high probability to phase separate and, in agreement with the above NMR results, Te phase separation is expected beyond the composition limit $Te_{0,625}Se$, namely $TeSe_{1,6}$. X-ray examination of the TeSe composition does not provide clear information on the presence of an additional c-Te due to phase separation. On the other hand, the "TeSe glass" is prepared in very fast quenching conditions, and it is highly probable that the excess of tellurium, compared to the formula predicted by NMR, is distributed as nanoparticles distributed in the glassy matrix. In other words, "TeSe glass" is probably a glass ceramic containing very fine grains difficult to detect by X-ray. Following this hypothesis, the model depicted in Figure 8 is valid except that the Te−Te fragments are now out of the chains and spread over in the glassy matrix. The examination of the T_g evaluation is also consistent with the Te-rich glasses having a very close T_g. It is also clear that the phase separation limit is dependent on the quenching conditions.

5. Conclusion

In the present work, the ^{125}Te and ^{77}Se solid-state NMR spectra are shown in the Te_xSe_{1-x} vitreous system. The ^{77}Se NMR spectra are unable to discriminate between three types of Se neighborhoods in the Te_xSe_{1-x} glass family at room temperature: Te-**Se**-Te, Se-**Se**-Te, and Se-**Se**-Se. Different models were considered to describe the structure: clustering process, homogeneous distribution, random distribution. Finally, it appears that Te and Se atoms are rather randomly distributed into the chains with nevertheless a preference for heteropolar bonds. There remains some doubt on the possibility that a small tellurium fragment could phase separate as nanoparticles beyond the $TeSe_{1,6}$, which is given by the NMR results as a kind of limit to the combination of tellurium and selenium atoms. Generally speaking, the ^{77}Se NMR spectra are very fruitful to understand the cross-behavior of Te and Se atoms. Compared to previous studies, the conclusion is different since for As_xSe_{1-x} glasses it has been shown that the $AsSe_3$ entities are homogeneously distributed ("chain-crossing model"),[10] whereas for Ge_xSe_{1-x} the presence of clusters constituted of $GeSe_4$ tetrahedra have to be considered.[9] These pioneer results on binary systems led to very fruitful information that will be essential for the future works on the ternary glasses such as TeAsSe or GeAsSe systems.

References and Notes

(1) Kokorina, V. F. In *Glasses for Infrared Optics*; Weber, M. J., Ed.; *Laser and Optical Science and Technology Series*; CRC Press: Boca Raton, 1996.

(2) Le Coq, D.; Boussard-Plédel, C.; Fonteneau, G.; Pain, T.; Bureau, B.; Adam, J. L. *Glass Technol.* **2003**, *44*(3), 132−136.

(3) Le Coq, D.; Michel, M.; Keirsse, J.; Boussard-Plédel, C.; Fonteneau, G.; Bureau, B.; Le Quéré, J. M.; Sire, O.; Lucas, J. *C. R. Chim.* **2003**, *5*, 1−7.

(4) Keirsse, J.; Boussard-Plédel, C.; Loréal, O.; Sire, O.; Bureau, B.; Leroyer, P.; Turlin, B.; Lucas, L. *Vib. Spectrosc.* **2003**, *32*(1), 23−32.

(5) Michel, K.; Bureau, B.; Boussard-Plédel, C.; Jouan, T.; Pouvreau, C.; Sangleboeuf, J. C.; Adam, J. L. *J. Non-Cryst. Solids* **2003**, *327*, 434−438.

(6) Quémard, C.; Smektala, F.; Couderc, V.; Barthélémy, A.; Lucas, J. *J. Phys. Chem. Solids* **2001**, *62*, 1435−1440.

(7) Boudebs, G.; Sanchez, F.; Troles, J.; Smektala, F. *Opt. Commun.* **2001**, *199*, 425−433.

(8) Troles, J.; Smektala, F.; Boudebs, G.; Monteil, A.; Bureau, B.; Lucas, J. *J. Optoelectron. Adv. Mater.* **2002**, *4*(3), 729−736.

(9) Bureau, B.; Troles, J.; Le Floch, M.; Guénot, P.; Smektala, F.; Lucas, J. *J. Non-Cryst. Solids* **2003**, *319*, 145−153.

(10) Bureau, B.; Troles, J.; Le Floch, M.; Smektala, F.; Silly, G.; Lucas, J. *Solid State Sci.* **2003**, *5*(1), 219−224.

(11) Bureau, B.; Troles, J.; Le Floch, M.; Guénot, P.; Smektala, F.; Lucas, J. *J. Non-Cryst. Solids* **2003**, *326*, 58−63.

(12) Rosenhahn, C.; Hayes, S.; Rosenhahn, B.; Eckert, E. *J. Non-Cryst. Solids* **2001**, *284*, 1.

(13) Maxwell, R.; Lathrop, D.; Eckert, H. *J. Non-Cryst. Solids* **1995**, *180*, 244.

(14) Duddeck, H. *Progr. NMR Spectrosc.* **1995**, *27*, 1.

(15) Orion, I.; Rocha, J.; Jobic, S.; Abadie, V.; Brec, R.; Fernandez, C.; Amoureux, J. P. *J. Chem. Soc.* **1997**, 3741−3748.

(16) Gabuda, S. P.; Kozlova, S. G.; Lapina, O. B.; Terskikh, V. V. *Chem. Phys. Lett.* **1998**, *282*, 245−249.

(17) Sakida, S.; Hayakawa, S.; Yoko, T. *J. Ceram. Soc. Jpn.* **1999**, *107*(5), 395−402.

(18) Hamard, C.; Auffret, V.; Pena, O.; Le Floch, M.; Nowak, B.; Wojakowski, A. *Physica B* **2000**, *291*, 339−349.

(19) Sakida, S.; Hayakawa, S.; Yoko, T. *J. Phys. Condens. Matter* **2000**, *12*, 2579−2595.

(20) Mizuno, K.; Magishi, K.; Shinonome, Y.; Saito, T.; Koyama, K.; Matsumoto, N.; Nagata, S. *Physica B* **2002**, *312*−*313*, 818−819.

(21) Massiot, D.; Farnan, I.; Gautier, N.; Trumeau, D.; Trokiner, A.; Coutures, J. P. *Solid State Nucl. Magn. Reson.* **1995**, *4*, 241.

(22) Grandinetti, P. J.; Baltisberger, J. H.; Llor, A.; Lee, Y. K.; Werner, U.; Eastmann, M. A.; Pines, A. *J. Magn. Reson.* **1993**, *A 103*, 72.

(23) Massiot, D.; Fayon, F.; Capron, F.; King, I.; Le Calvé, S.; Alonso, B.; Durand, J. O.; Bujoli, B.; Gan, Z.; Hoatson, G. *Magn. Reson. Chem.* **2002**, *40*, 70.

(24) Adenis, C.; Langer, V.; Lindqvist, O. *Acta Crystallogr., C* **1989**, *45*, 941.

(25) Günther, B.; Kanert, O. *Phys. Rev. B* **1985**, *31*, 20.